DOE STTR Phase I:
Hybrid Nanocrystalline Permanent Magnets for Beam Focusing in High Energy Accelerators

July 2005

Final Report for
Grant No. DE-FG0204ER86185

For Period of 13 July 2004 through 12 April 2005

Prepared by:

Mr. Youngson He,
FutureTek USA Corp.
2705 Far Hills, Dayton, OH 45419

and

Sam Liu
University of Dayton Research Institute
300 College Park, Dayton, Ohio 45469-0174

d. Rights to SBIR/STTR Data.

(1) The grantee is authorized to affix the following SBIR/STTR Rights Notice to SBIR/STTR data delivered under this grant and the Government will thereafter treat the data, subject to the provisions of paragraphs e. and f. of this term, in accordance with such Notice:

SBIR/STTR RIGHTS NOTICE

These SBIR/STTR data are furnished with SBIR/STTR rights under Grant No. DE-FG0204ER86185 For a period of 4 years after acceptance of all items to be delivered under this grant, the Government agrees to use these data for Government purposes only, and they shall not be disclosed outside the Government (including disclosure for procurement purposes) during such period without permission of the grantee, except that, subject to the foregoing use and disclosure prohibitions, such data may be disclosed for use by support contractors. After the aforesaid 4-year period the Government has a royalty-free license to use, and to authorize others to use on its behalf, these data for Government purposes, but is relieved of all disclosure prohibitions and assumes no liability for unauthorized use of these data by third parties. This Notice shall be affixed to any reproductions of these data in whole or in part.

REPORT DOCUMENTATION PAGE

Form Approved
OMB No. 0704-0188

1. REPORT DATE *(DD-MM-YYYY)*	2. REPORT TYPE	3. DATES COVERED *(From - To)*
July 2005	Final Report	13 June 2004 through 12 April 2005

4. TITLE AND SUBTITLE

Hybrid Nanocrystalline Permanent Magnets for Beam Focusing in High Energy Accelerators

5a. CONTRACT NUMBER

5b. GRANT NUMBER
DE-FG0204ER86185

5c. PROGRAM ELEMENT NUMBER

6. AUTHOR(S)

Sam Liu

5d. PROJECT NUMBER

5e. TASK NUMBER

5f. WORK UNIT NUMBER

7. PERFORMING ORGANIZATION NAME(S) AND ADDRESS(ES)

University of Dayton Research Institute
300 College Park Ave.
Dayton, OH 45469

FutureTek USA Corp.
2705 Far Hills Ave.
Dayton, OH 45419

8. PERFORMING ORGANIZATION REPORT NUMBER

FTC-UDR-TR-2005-00154

9. SPONSORING / MONITORING AGENCY NAME(S) AND ADDRESS(ES)

U.S. Department of Energy / ACQ
Chicago Office
9800 South Office
Argonne, IL 60439

10. SPONSOR/MONITOR'S ACRONYM(S)

11. SPONSOR/MONITOR'S REPORT NUMBER(S)

12. DISTRIBUTION / AVAILABILITY STATEMENT

Prior approval required by Sponsor for distribution

13. SUPPLEMENTARY NOTES

14. ABSTRACT

In this DoE 2004 STTR Phase I research project, bulk hybrid nanograin $Nd_2Fe_{14}B/Sm_2(Co,Fe)_{17}$ magnets with ${}_MH_c$ = 14.2 kOe and $(BH)_{max}$ = 27.3 MGOe were successfully synthesized. In addition, bulk nanograin $PrCo_5$ magnets with ${}_MH_c$ over 15 kOe and bulk hybrid anisotropic nanocomposite $Pr_2(Fe,Co)_{14}B/Pr(Co,Fe)_5$ and $Pr_2(Fe,Co)_{14}B/Pr_2(Co,Fe)_{17}$ magnets with $(BH)_{max}$ of 28 to 35 MGOe were synthesized. These efforts were guided by the novel model of coercivity mechanism in nanograin magnetic materials and through the use of the innovative rapid RF inductive hot compaction process. With further R&D, a new class of permanent magnets that have the same level of magnetic performance as the mainstream sintered Nd-Fe-B magnets with $(BH)_{max}$ = 35 to 45 MGOe and much improved thermal stability will be developed.

15. SUBJECT TERMS

High temperature, hybrid magnets, Nd-Fe-B, Sm-Co, Pr-Co, temperature coefficient, thermal stability

16. SECURITY CLASSIFICATION OF:			17. LIMITATION OF ABSTRACT	18. NUMBER OF PAGES	19a. NAME OF RESPONSIBLE PERSON
					Sam Liu
a. REPORT	b. ABSTRACT	c. THIS PAGE	SAR	29	19b. TELEPHONE NUMBER *(include area code)*
Unclassified	Unclassified	Unclassified			(937) 229-3272

Standard Form 298 (Rev. 8-98)
Prescribed by ANSI Std. Z39.18

ABSTRACT

In this DoE 2004 STTR Phase I research project, bulk hybrid nanograin $Nd_2Fe_{14}B/Sm_2(Co,Fe)_{17}$ magnets with ${}_MH_c$ = 14.2 kOe and $(BH)_{max}$ = 27.3 MGOe were successfully synthesized. In addition, bulk nanograin $PrCo_5$ magnets with ${}_MH_c$ over 15 kOe and bulk hybrid anisotropic nanocomposite $Pr_2(Fe,Co)_{14}B/Pr(Co,Fe)_5$ and $Pr_2(Fe,Co)_{14}B/Pr_2(Co,Fe)_{17}$ magnets with $(BH)_{max}$ of 28 to 35 MGOe were synthesized. These efforts were guided by the novel model of coercivity mechanism in nanograin magnetic materials and through the use of the innovative rapid RF inductive hot compaction process. With further R&D, a new class of permanent magnets that have the same level of magnetic performance as the mainstream sintered Nd-Fe-B magnets with $(BH)_{max}$ = 35 to 45 MGOe and much improved thermal stability will be developed.

TABLE OF CONTENTS

LIST OF FIGURES

LIST OF FIGURES (Concluded)

LIST OF TABLES

ACKNOWLEDGEMENTS

This research was supported by DoE/FutureTek under Grant No. DE-FG02-04ER86185.

1. Introduction

1.1 Radiation damage of permanent magnets

A magnetic field is used for beam focusing in high-energy accelerators. For this purpose, electromagnets, hard ferrite, Sm-Co, or Nd-Fe-B magnets can be utilized. The advantages of using permanent magnets include zero operating costs and reduced capital costs by eliminating power supplies. The main disadvantage is the loss of strength of the magnets due to radiation damage. According to J.T. Volk [1], permanent magnets with high Curie temperature, small grains, and high intrinsic coercivity demonstrate better radiation resistance. Recent experiments performed by the University of Dayton Magnetics Laboratory, Electron Energy Corporation, and the Ohio State University have revealed that the nature of the radiation damage of a permanent magnet is virtually the thermal demagnetization caused by temperature rise inside the magnet when it is subjected to radiation [2]. Therefore, even though a high-energy accelerator may operate in a room temperature environment, the magnet itself can be actually operating at elevated temperatures under radiation. For example, according to ref. [2], under the neutron flux of $1x10^{13}$ neu/cm^2·sec, the temperature inside a Nd-Fe-B magnet can reach 170°C. Consequently, permanent magnets with improved thermal stability must be used for beam focusing in high-energy accelerators.

1.2 Limitations of conventional sintered Nd-Fe-B magnets and approaches to improving their thermal stability

Permanent magnet materials that combine high magnetic performance and excellent thermal stability are required for beam focusing in high-energy accelerators. However, no single existing magnet material can completely satisfy these requirements. Table 1 lists a comparison of different types of permanent magnets. It can be seen from Table 1 that hard ferrite magnets have the lowest magnetic performance, an intermediate Curie temperature, and a very low price. On the other hand, $Sm_2(Co,Fe,Cu,Zr)_{17}$ magnets have the highest Curie temperature of around 800°C, moderately high magnetic performance, and a high price; while mainstream Nd-Fe-B magnets demonstrate the highest room temperature magnetic performance, but the lowest Curie temperature of 310°C.

Table 1. A Comparison of Different Types of Permanent Magnets

Magnets	$4\pi M_s$ (kG)	$_MH_c$ (kOe)	$(BH)_{max}$ (MGOe)	T_C (°C)	Highest Operating Temperature (°C)	Price
Hard ferrite	3 - 4	2 - 3	3 - 4	450	180	Very
$Sm_2(Co,Fe,Cu,Zr)_{17}$	11 - 12	20 - 30	20 - 28	800	300 - 550	High
Mainstream $Nd_2Fe_{14}B$	12 - 15	10 - 15	35 - 45	310	80	Medium
Elevated temperature $(Nd,Dy,Tb)_2(Fe,Co)_{14}B$	10 - 11	20 - 30	28 - 35	350	150	Higher

Apparently, a wide gap in the operating temperature exists between the $Sm_2(Co,Fe,Cu,Zr)_{17}$ magnets and mainstream Nd-Fe-B magnets. Further, because of their low Curie temperature, Nd-Fe-B magnets have very large negative temperature coefficients of magnetic properties, thus, very poor thermal stability. The operating temperature gap between $Sm_2(Co,Fe,Cu,Zr)_{17}$ and mainstream Nd-Fe-B (80 to 300°C) is a precisely very critical temperature range for many important applications, such as for beam focusing, magnetic sensors, and automobiles.

Though Nd-Fe-B magnets have excellent magnetic performance at room temperature, their magnetic properties, especially intrinsic coercivity, drop sharply with increasing temperature. To deal with this problem, small amounts of heavy rare earths Dy and Tb have been used to substitute for Nd, leading to Nd-Dy-Tb-Fe-B magnets with high coercivity.

Partially substituting Co for Fe in Nd-Fe-B magnets can effectively increase their Curie temperature, but deteriorate coercivity and, thus, increase the irreversible loss of magnetic strength at elevated temperature. Combining these two approaches, magnets based on $(Nd,Dy,Tb)_2(Fe,Co)_{14}B$ demonstrate improved thermal stability and can be used at temperatures up to 150°C. However, because the magnetic coupling between heavy rare earths (Dy and Tb) and 3d-transition metals (Fe and Co) are anti-parallel, adding Dy and Tb significantly decreases magnetization and magnetic performance. As shown in Table 1, magnets based on $(Nd,Dy,Tb)_2(Fe,Co)_{14}B$ for elevated temperature applications have a $(BH)_{max}$ of only 28 to 35 MGOe. On the other hand, both Dy and Tb are very expensive, which significantly increases the magnet cost.

The third approach is to make hybrid $Nd_2Fe_{14}B/Sm_2(Co,Fe,Cu,Zr)_{17}$ magnets that may combine the high magnetic performance of $Nd_2Fe_{14}B$ and excellent high temperature stability of $Sm_2(Co,Fe,Cu,Zr)_{17}$. Unfortunately, there are at least two technical difficulties in making this good idea a reality.

(a) Incompatible processes

The process of making sintered Nd-Fe-B magnets is not compatible with the process of making sintered $Sm_2(Co,Fe,Cu,Zr)_{17}$ magnets.

- The process of making sintered $Nd_2Fe_{14}B$-based magnets is relatively simple. It includes melting, crushing, milling, powder alignment and compaction, sintering at around 1080°C for 1 to 2 hours followed by an anneal at around 600°C for 1 hour.
- Sintered $Sm_2(Co,Fe,Cu,Zr)_{17}$ magnets are prepared with a very complex process. After compaction, the green bodies must be sintered at a high temperature of 1200°C to reach full density. This sintering temperature is higher than the melting point of $Nd_2Fe_{14}B$. After the sintering, a complex and long-term heat treatment procedure must be performed and the entire process lasts for about 3 days.

(b) Interdiffusion between two different types of materials at elevated temperatures

The interdiffusion between $Nd_2Fe_{14}B$ and $Sm_2(Co,Fe,Cu,Zr)_{17}$ will take place during sintering and heat treatment at elevated temperatures. The possible products from the interdiffusion include $Sm_2Fe_{14}B$, Nd_2Co_{17}, $Nd_2Co_{14}B$, and Sm_2Fe_{17}. Unfortunately, most of these products ($Sm_2Fe_{14}B$, Nd_2Co_{17}, and Sm_2Fe_{17}) have unfavorable easy basal plane anisotropy and, hence, a very low anisotropy field, which leads to very low coercivity.

2. Technical Approach in This STTR Phase I Research Project

In order to resolve problems associated with the conventional sintered Nd-Fe-B magnets and conventional Nd-Fe-B/$Sm_2(Co,Fe,Cu,Zr)_{17}$ magnets, the FutureTek/University of Dayton research team's technical approach was to make a new class of novel hybrid nanograin $Nd_2Fe_{14}B/Sm_2(Co,Fe)_{17}$ and $Nd_2Fe_{14}B/PrCo_5$ permanent magnets for beam focusing in high-energy accelerators and for many other applications where better thermal stability and/or higher operating temperatures are needed as compared with the current Nd-Fe-B magnets. These hybrid nanograin permanent magnets will incorporate the high Curie temperature and excellent thermal stability of the Sm-Co or Pr-Co based magnets and high magnetization of the Nd-Fe-B magnets and will fill the gap between these two types of conventional magnet materials.

This new class of magnets was studied under the guidance of the innovative concept of coercivity in magnetic materials possessing nanograin structure proposed by Prof. Sam Liu of the University of Dayton [3, 4]. The hybrid nanograin magnets were synthesized using melt spinning followed by the innovative technologies of rapid hot compaction and hot deformation developed recently by the University of Dayton Magnetics Lab[5, 6]. Applying these innovative technologies, all technical difficulties in making conventional hybrid magnets with micron grains were readily overcome.

3. Scientific Basis of the Technical Approach

A fundamental change takes place in the coercivity mechanism of magnetic materials when their grain size is reduced from a conventional micrometer to a nanometer range. A convincing example is the Sm_2Co_{17} compound. Though the Sm_2Co_{17} compound has a high anisotropy field of 65 kOe, useful intrinsic coercivity (> 8 kOe) could not be developed in it. Actually, it took more than 10 years (1970 - 1983) for researchers to modify the compositions (by adding Cu, Zr, and extra Sm) and to develop a complex sintering and heat-treatment procedure for achieving useful coercivity (> 8 kOe). The procedure consists of high-temperature sintering at ≥ 1200°C for 1 to 2 hours, a solid solution heat treatment at around 1080°C for 3 to 5 hours, and a very long aging period at ~800°C for 30 to 50 hours, followed by a very slow cooling period from 800°C to 400°C at 1 to 2°C/minute. The whole procedure takes three days to complete. These compositional modifications and heat treatments are required to form a fine-scale cellular microstructure, in which the cell boundary phase has low anisotropy and serves as pinning sites for domain wall motion, leading to high coercivity [7-9].

In contrast, a study at the University of Dayton revealed that annealing an amorphous stoichiometric Sm_2Co_{17} at 700°C for only 1 minute resulted in similar or even higher coercivity (> 15 kOe) [10]! Based on many novel phenomena observed in magnetic materials having nanograin structure, Prof. Sam Liu of the University of Dayton proposed an innovative coercivity model [3, 4]. The principal points of this new model are listed below.

- In magnetic materials with nanograins, the formation of multiple magnetic domains in a grain is no longer energetically favorable.
- The magnetization reversal in nanograin magnetic materials is not carried out by nucleation of reversed magnetic domains or domain wall motion.

- The magnetization reversal in nanograin magnetic materials is carried out by rotation of magnetization. The interface exchange coupling makes it an incoherent rotation.
- In magnetic materials with nanograin structure, there is no longer a need to create a specific microstructure to prevent the formation of reversed magnetic domains or to restrict domain wall motion.
- High uniaxial magnetocrystalline anisotropy is not only a necessary condition for high coercivity, as it is in magnetic materials with micrograins, it is also the sufficient condition for high coercivity in magnetic materials with nanograins.
- A direct connection between coercivity and magnetocrystalline anisotropy is established in magnetic materials with nanograin structure.
- Consequently, high coercivity should be readily obtained for any magnetic materials that have high uniaxial anisotropy, provided that the materials possess nanograin structure.

The basic idea of this new coercivity model is illustrated in Figure 1.

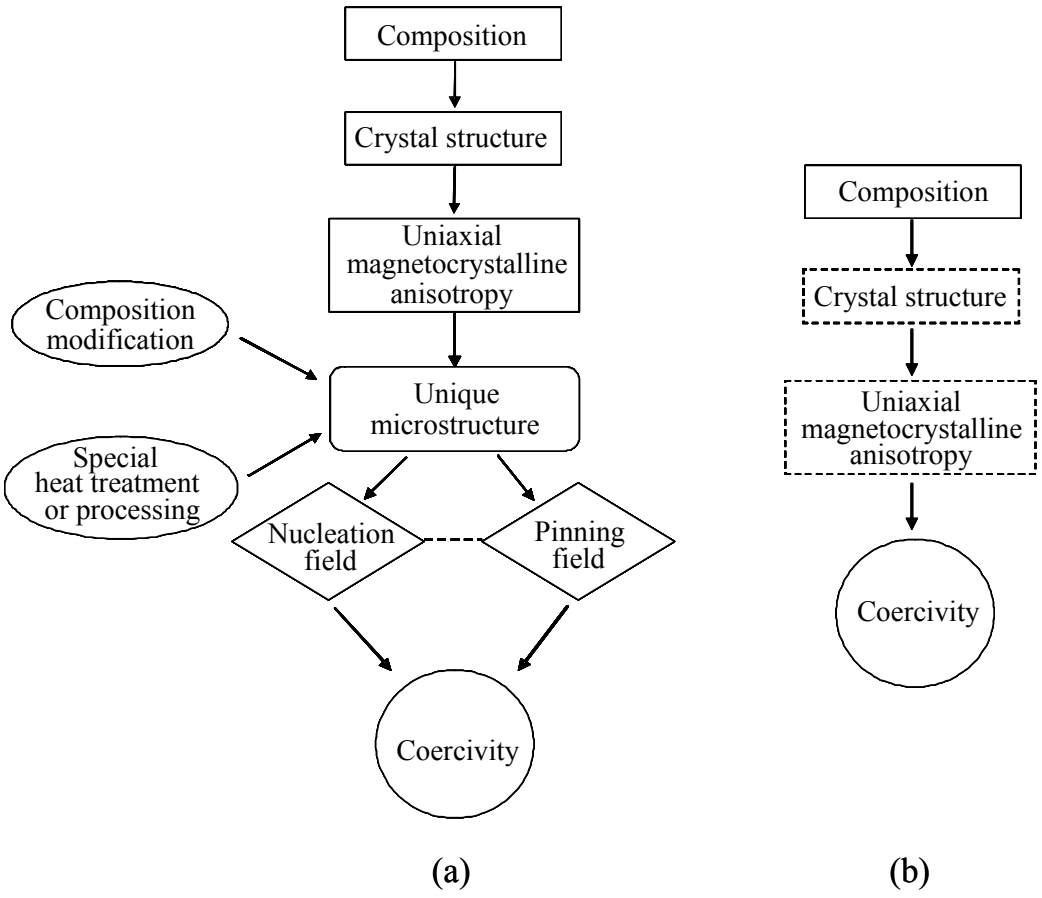

Figure 1. Coercivity mechanisms in rare earth permanent magnets with micron grains (a) and nanograins (b).

The new coercivity model has been verified and supported by many experimental results. For example, a high coercivity of 12 kOe was easily obtained in a nanograin YCo_5 compound after annealing an amorphous YCo_5 at 750°C for 2 minutes. It is well known that YCo_5 was the first rare earth-transition metal compound that was discovered to have very high anisotropy field of 130 kOe [11]; however, useful coercivity could not be obtained in a conventional YCo_5 with micrometer grains. More recently, Ms. Shen of FutureTek, PI of the proposed project, successfully obtained high coercivity of 16 kOe in a bulk nanograin $PrCo_5$ magnet in this STTR Phase I project (refer to Figure 10). Again, high coercivity is difficult to achieve in $PrCo_5$ with micrometer grain structure. Successfully obtaining high coercivity in nanograin $PrCo_5$ makes it possible to synthesize hybrid nanocrystalline $Pr_2(Co,Fe)_{14}B/Pr(Co,Fe)_5$ magnets.

4. Experimental Results and Discussions

The technical objective of the STTR Phase I research effort was to demonstrate the feasibility of an innovative idea of synthesizing a new class of hybrid nanocrystalline permanent magnets, such as $Nd_2(Fe,Co)_{14}B/Sm_2(Co,Fe)_{17}$, for beam focusing in high-energy accelerators and for many other applications where better thermal stability and/or higher operating temperature is needed.

This Phase I objective has been completely and successfully accomplished. In addition to the originally-planned hybrid nanocrystalline $Nd_2(Fe,Co)_{14}B/Sm_2(Co,Fe)_{17}$ permanent magnets, FutureTek/University of Dayton researchers have successfully synthesized hybrid magnets based on a new $Pr_2(Fe,Co)_{14}B/Pr(Co,Fe)_5$ composite alloy system, which demonstrates superior magnetic performance, a significantly wide processing window, and lower material cost as compared to the $Nd_2(Fe,Co)_{14}B/Sm_2(Co,Fe)_{17}$ system.

The Phase I research project has successfully established that synthesizing a hybrid nanocrystalline two-phase permanent magnet that combine the high magnetic performance of one phase and superior thermal stability of another phase by using the innovative inductive rapid hot press and hot deformation technologies is highly feasible.

The Phase I project has clearly established that with further R&D, a new class of hybrid nanocrystalline magnets with significant commercial potential can be developed. These new permanent magnets will be ideal for beam focusing in high-energy accelerators and in many other critical DoE applications such as magnetic sensors and automobiles, especially for hybrid and fuel-cell powered automobiles and other vehicles. In addition, an abnormal coercivity enhancement was observed during the Phase I research, which may provide clues for new materials development.

More detailed descriptions of the Phase I accomplishments are given in the following subsections.

4.1 Hybrid nanocrystalline $Nd_2(Fe,Co)_{14}B/Sm_2(Co,Fe)_{17}$ magnets

Hybrid nanocrystalline $Nd_2(Fe,Co)_{14}B/Sm_2(Co,Fe)_{17}$ magnets have been successfully synthesized and characterized during the STTR Phase I project. Figure 2 shows a demagnetization curve of a hybrid nanocrystalline $Nd_2(Fe_{0.94}Co_{0.06})_{14}B/Sm_2(Co_{0.7}Fe_{0.3})_{17}$ [80 wt%/20 wt%] magnet. This magnet was made using a process including melting, melt spinning, crushing and powder blending, inductive rapid hot press, and hot deformation.

As a comparison, a demagnetization curve of a conventional hybrid $Nd_{15}Fe_{79}B_6$/ $Sm(Co_{0.745}Fe_{0.15}Cu_{0.08}Zr_{0.025})_{7.4}$ [80 wt%/20 wt%] magnet is also given. This magnet was prepared using a process including melting, crushing, ball milling, fine powder blending, inductive hot press, and hot deformation. It can be seen from Figure 2 that the hybrid nanocrystalline magnet demonstrates a high B_r of 10.99 kG, a high $_MH_c$ of 14.26 kOe, and a high $(BH)_{max}$ of 27.36 MGOe, while the conventional hybrid magnet shows very poor magnetic performance of B_r = 2.54 kG, $_MH_c$ = 0.39 kOe, and $(BH)_{max}$ = 0.24 MGOe. Apparently, incompatible processing of two materials and interdiffusion between two materials are responsible for the poor magnetic performance of the conventional hybrid magnet.

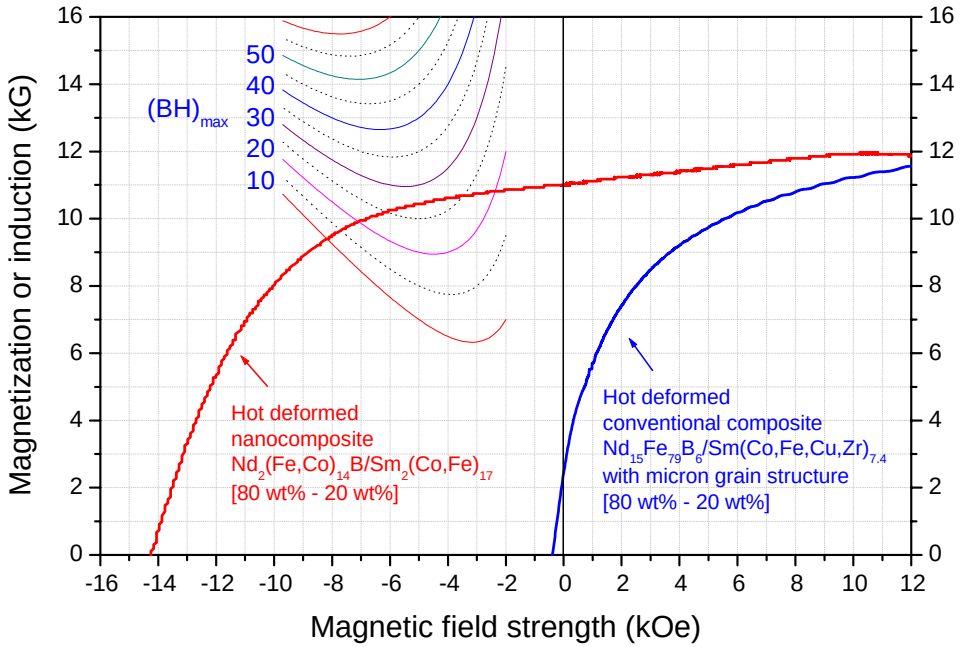

Fig. 2. Demagnetization curves of a hot deformed hybrid nanocrystalline $Nd_2(Fe_{0.94}Co_{0.06})_{14}B/Sm_2(Co_{0.7}Fe_{0.3})_{17}$ magnet and a hot deformed conventional hybrid $Nd_{15}Fe_{79}B_6/Sm(Co_{0.745}Fe_{0.15}Cu_{0.08}Zr_{0.025})_{7.4}$ magnet. Both magnets contain 80 wt% Nd-Fe-B and 20 wt% Sm-Co.

Even though a moderately high $(BH)_{max}$ of over 27 MGOe was obtained in the hybrid $Nd_2(Fe,Co)_{14}B/Sm_2(Co,Fe)_{17}$ magnet, achieving $_MH_c$ over 10 kOe is not always easy. If the hot press and hot deformation are not made fast enough, the obtained coercivity will be lower than 10 kOe. Apparently, this is the outcome of interdiffusion.

Figure 3 illustrates the temperature coefficient of magnetic flux versus temperature for a $Nd_2(Fe_{0.94}Co_{0.06})_{14}B$, a $Sm_2(Co_{0.7}Fe_{0.3})_{17}$ and two hybrid $Nd_2(Fe_{0.94}Co_{0.06})_{14}B$/ $Sm_2(Co_{0.7}Fe_{0.3})_{17}$ magnets. Assuming that a temperature coefficient of not worse than -0.10%/°C is required for a particular application, to satisfy this requirement, the highest operating temperature for $Nd_2(Fe_{0.94}Co_{0.06})_{14}B$ is only 25°C. The operating temperatures can be increased to 150 and 200°C, respectively, if the hybrid $Nd_2(Fe_{0.94}Co_{0.06})_{14}B$/ $Sm_2(Co_{0.7}Fe_{0.3})_{17}$ [80 wt%/20 wt%] and $Nd_2(Fe_{0.94}Co_{0.06})_{14}B/Sm_2(Co_{0.7}Fe_{0.3})_{17}$ [60 wt%/40 wt%] are used.

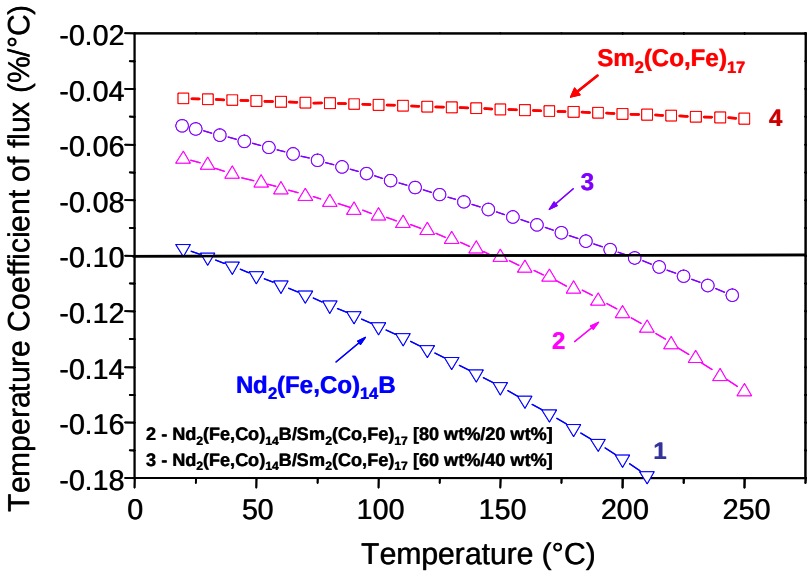

Fig. 3. Temperature coefficient of magnetic flux vs. temperature for (1) $Nd_2(Fe_{0.94}Co_{0.06})_{14}B$; (2) hybrid $Nd_2(Fe,Co)_{14}B/Sm_2(Co,Fe)_{17}$ [80 wt%/20 wt%]; (3) hybrid $Nd_2(Fe_{0.94}Co_{0.06})_{14}B/Sm_2(Co_{0.7}Fe_{0.3})_{17}$ [60 wt%/40 wt%]; and (4) $Sm_2(Co_{0.7}Fe_{0.3})_{17}$). All magnets have L/D = 1.

Figure 4 demonstrates the temperature dependence of intrinsic coercivity, ${}_MH_c$, of a hybrid nanocrystalline $Nd_2(Fe_{0.94}Co_{0.06})_{14}B/Sm_2(Co_{0.7}Fe_{0.3})_{17}$ [60 wt%/40 wt%] magnet. Since it is a two-phase material with one component having a low Curie temperature of 310°C and another component with a high Curie temperature of 840°C, one may expected a kinked ${}_MH_c$-T curve. However, as shown in Figure 4, a very smooth ${}_MH_c$-T curve was obtained. Obviously, this is the outcome of the interface exchange coupling interaction between the two phases.

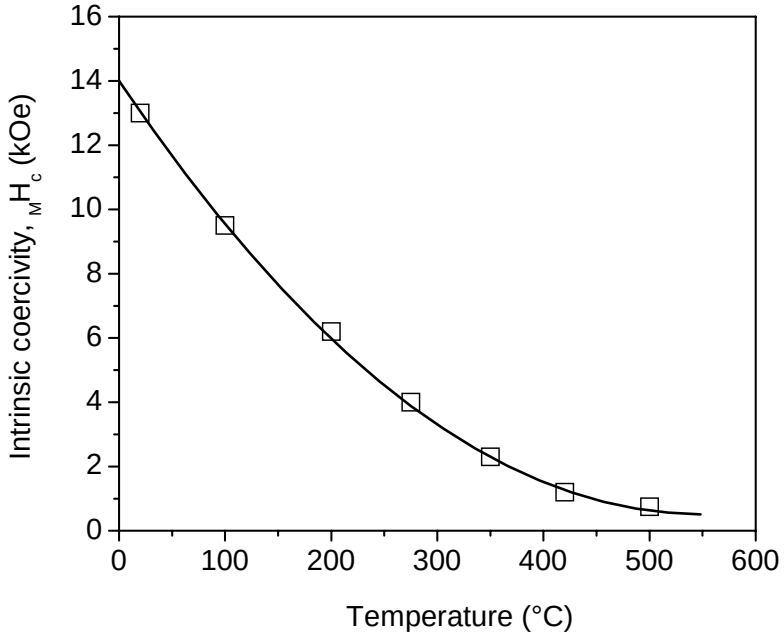

Fig. 4. Temperature dependence of intrinsic coercivity of a hybrid nanocrystalline $Nd_2(Fe_{0.94}Co_{0.06})_{14}B/Sm_2(Co_{0.7}Fe_{0.3})_{17}$ [60 wt%-40 wt%] magnet.

A micrograph showing the fracture surface of a hot deformed anisotropic hybrid nanocrystalline $Nd_2(Fe_{0.94}Co_{0.06})_{14}B/Sm_2(Co_{0.7}Fe_{0.3})_{17}$ [80 wt%-20 wt%] magnet is given in Figure 5. This micrograph demonstrates the grain alignment after hot deformation. Figure 6 shows microstructures of a hybrid $Nd_2(Fe_{0.94}Co_{0.06})_{14}B/Sm_2(Co_{0.7}Fe_{0.3})_{17}$ [80 wt%-20 wt%] magnet observed using scanning electron microscopy (SEM). The micro-compositions were determined using energy dispersed spectrum (EDS) and the results are given in Figure 7. It can be clearly observed from Figure 6(a) that the microstructure of the hybrid $Nd_2(Fe_{0.94}Co_{0.06})_{14}B/Sm_2(Co_{0.7}Fe_{0.3})_{17}$ magnet consists of three distinguished zones. Among them, Zone 1 (matrix) is $Nd_2(Fe,Co)_{14}B$ as revealed by EDS (Figure 7); Zone 2 is $Sm_2(Co,Fe)_{17}$; while Zone 3 is the interdiffusion area between $Nd_2(Fe,Co)_{14}B$ and $Sm_2(Co,Fe)_{17}$.

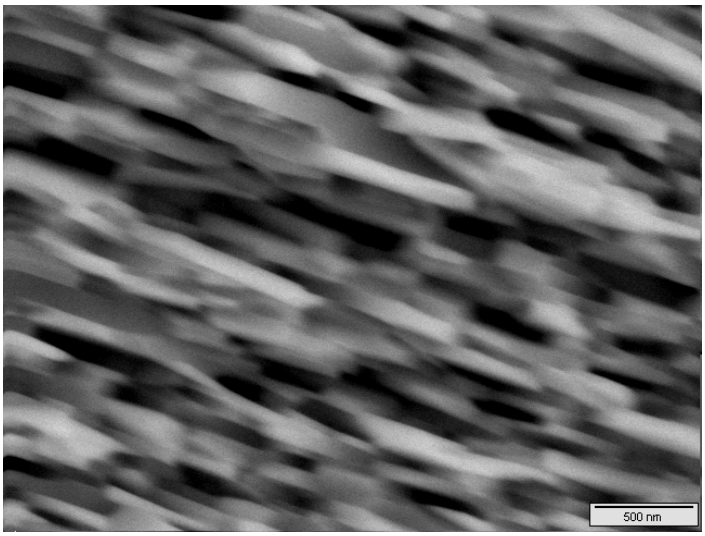

Fig. 5. SEM micrograph of the fracture surface of a hot deformed hybrid nanocrystalline $Nd_2(Fe_{0.94}Co_{0.06})_{14}B/Sm_2(Co_{0.7}Fe_{0.3})_{17}$ [80 wt%-20 wt%] magnet.

The SEM analysis also revealed that the $Nd_2(Fe,Co)_{14}B$ area (Zone 1) has elongated and aligned grains as shown in Figure 6(b), while both the $Sm_2(Co,Fe)_{17}$ area (Zone 2) and the interdiffusion area (Zone 3) are characterized as very fine equiaxial grains without grain alignment. These results indicate that in a hybrid nanocrystalline $Nd_2(Fe,Co)_{14}B/$ $Sm_2(Co,Fe)_{17}$ magnet, only the $Nd_2(Fe,Co)_{14}B$ component can be made anisotropic by creating grain alignment during the hot deformation, while the $Sm_2(Co,Fe)_{17}$ component remains basically isotropic. This observation is in good agreement with results of other recent studies in which it was shown that grain alignment is difficult to obtain by hot deformation in nanostructure $Sm_2(Co,Fe)_{17}$ magnet [12,13]. Because of this limitation, achieving $(BH)_{max}$ greater than 30 MGOe in the $Nd_2(Fe,Co)_{14}B/Sm_2(Co,Fe)_{17}$ system would be difficult.

To investigate the long-term thermal stability of the hybrid magnet, a $Nd_2(Fe_{0.94}Co_{0.06})_{14}B/$ $Sm_2(Co_{0.7}Fe_{0.3})_{17}$ [80 wt%-20 wt%] magnet with L/D = 1 was aged at 100°C in air and the result is given in Figure 8. It can be seen from Figure 8 that the normalized magnetic flux remains the same at 100°C over 5000 hours, indicating no interdiffusion between the two components of the hybrid magnet at 100°C.

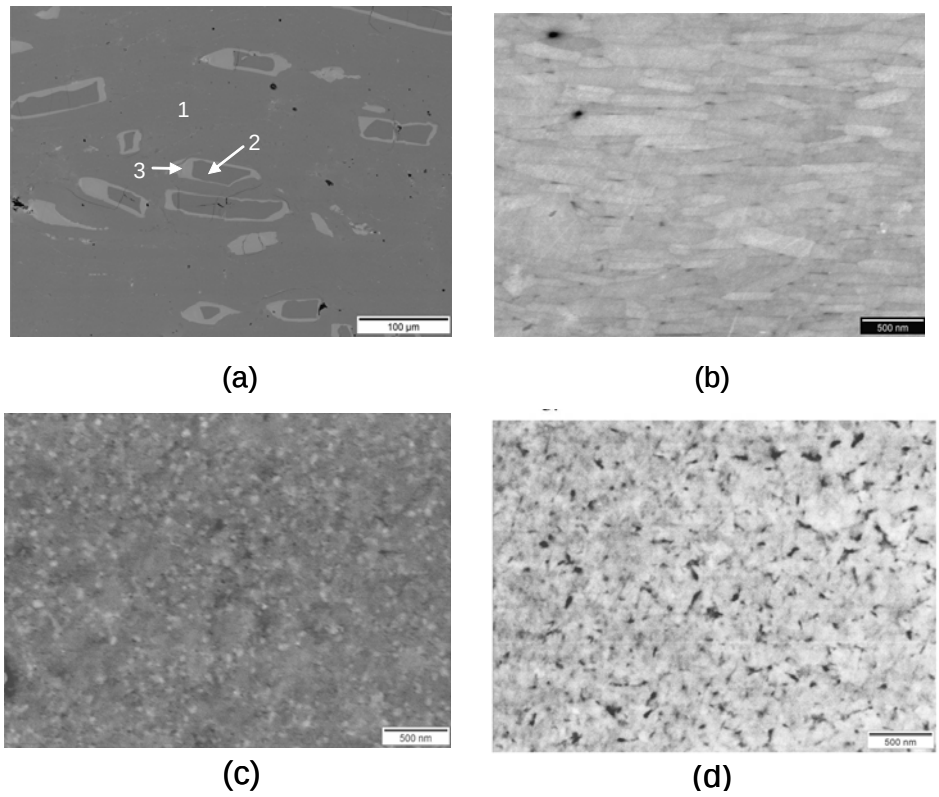

Fig. 6. SEM micrographs of a nanocomposite $Nd_2(Fe_{0.94}Co_{0.06})_{14}B/Sm_2(Co_{0.7}Fe_{0.3})_{17}$ [80 wt%-20 wt%] magnet showing three zones: Zone 1 – $Nd_2(Fe,Co)_{14}B$ matrix (a and b); Zone 2 – $Sm_2(Co,Fe)_{17}$ (c); Zone 3 – diffusion zone between two phases (d).

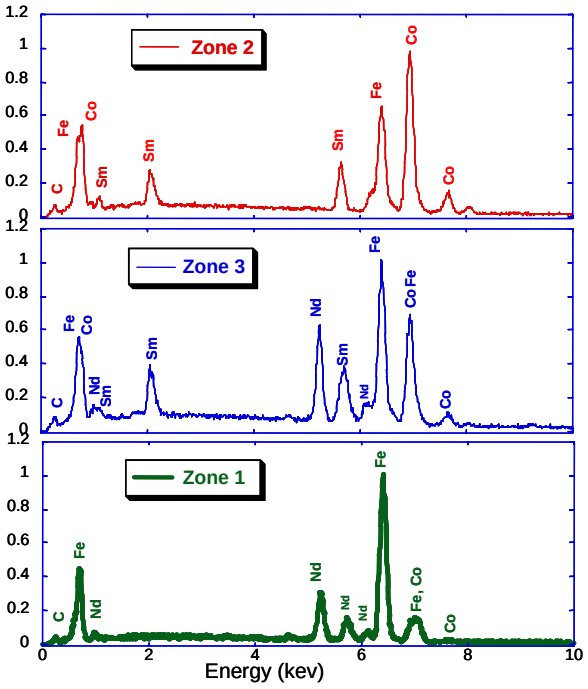

Fig. 7. Results of EDS analysis for hybrid nanocrystalline $Nd_2(Fe_{0.94}Co_{0.06})_{14}B/Sm_2(Co_{0.7}Fe_{0.3})_{17}$ [80 wt%-20 wt%] magnet.

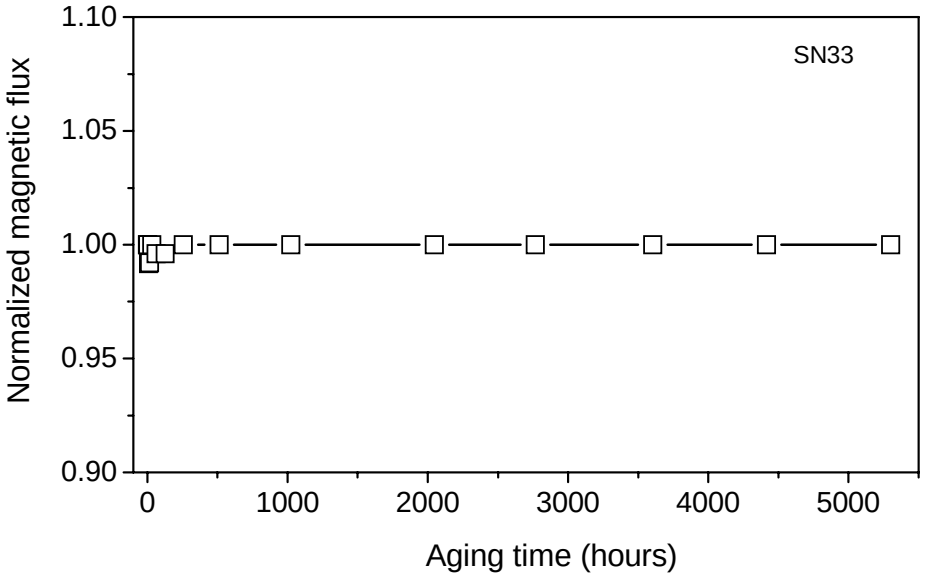

Fig. 8. Result of a long-term aging experiment of a nanocrystalline $Nd_2(Fe_{0.94}Co_{0.06})_{14}B/Sm_2(Co_{0.7}Fe_{0.3})_{17}$ [80 wt%-20 wt%] magnet with L/D = 1 aged at 100°C in air.

4.2 Hybrid nanocrystalline $Pr_2(Fe,Co)_{14}B/Pr(Co,Fe)_5$ magnets

Realizing the limitation of the $Nd_2(Fe,Co)_{14}B/Sm_2(Co,Fe)_{17}$ hybrid system, a new hybrid system of $Pr_2(Fe,Co)_{14}B/Pr(Co,Fe)_5$ has been studied during the second half of the STTR Phase I project. Because both 2:14:1 and 1:5 phases have the same rare earth and similar transition metals in this system, even as interdiffusion takes place at elevated temperatures, the magnetic performance of the hybrid magnet will not be affected.

In the Phase I project, single $Pr_2(Fe,Co)_{14}B$ and $Pr(Co,Fe)_5$ magnets were first studied separately, and efforts were then made to synthesize hybrid nanocrystalline $Pr_2(Fe,Co)_{14}B/Pr(Co,Fe)_5$ magnets. Figure 9 shows demagnetization curves of the first hot pressed $Pr_2(Fe_{0.94}Co_{0.06})_{14}B$ specimen and magnetization curves of the same magnet after 70% hot deformation at 900°C. It can be seen that the hot deformed anisotropic $Pr_2(Fe_{0.94}Co_{0.06})_{14}B$ magnet demonstrates very high intrinsic coercivity over 17 kOe, very good squareness of the demagnetization curve, and high $(BH)_{max}$ over 33 MGOe.

Figure 10 shows demagnetization curves of the first hot pressed $PrCo_5$ specimen and magnetization curves of the same magnet after 70% hot deformation at 900°C. After the hot deformation, B_r increased from 7.09 to 8.39 kG, ${}_MH_c$ decreased from 15.33 to 9.18 kOe, and $(BH)_{max}$ increased from 11.52 to 16.77 MGOe. Apparently, at least partial grain alignment was created during hot deformation. This is the result of our very first specimen. With further improvements in alloy composition and processing parameters, much better results can be obtained. Because the magneto-crystalline anisotropy field of $PrCo_5$ is 170 kOe, much higher than that of $Pr_2Fe_{14}B$ (75 kOe), much higher coercivity can be developed in $PrCo_5$-based nanograin magnets.

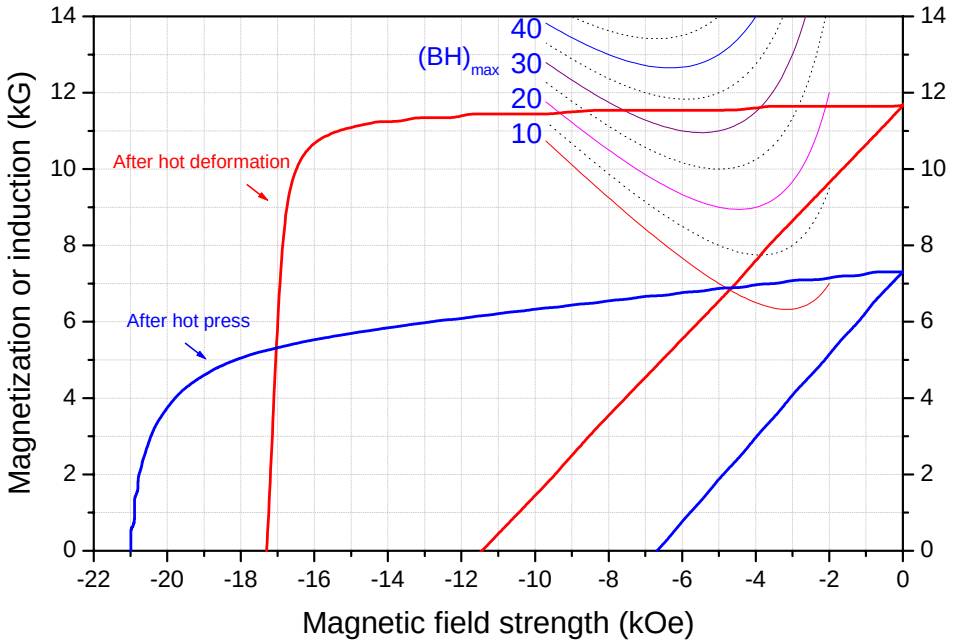

Fig. 9. Demagnetization curves of hot pressed isotropic $Pr_2(Fe_{0.94}Co_{0.06})_{14}B$ and hot deformed anisotropic $Pr_2(Fe_{0.94}Co_{0.06})_{14}B$.

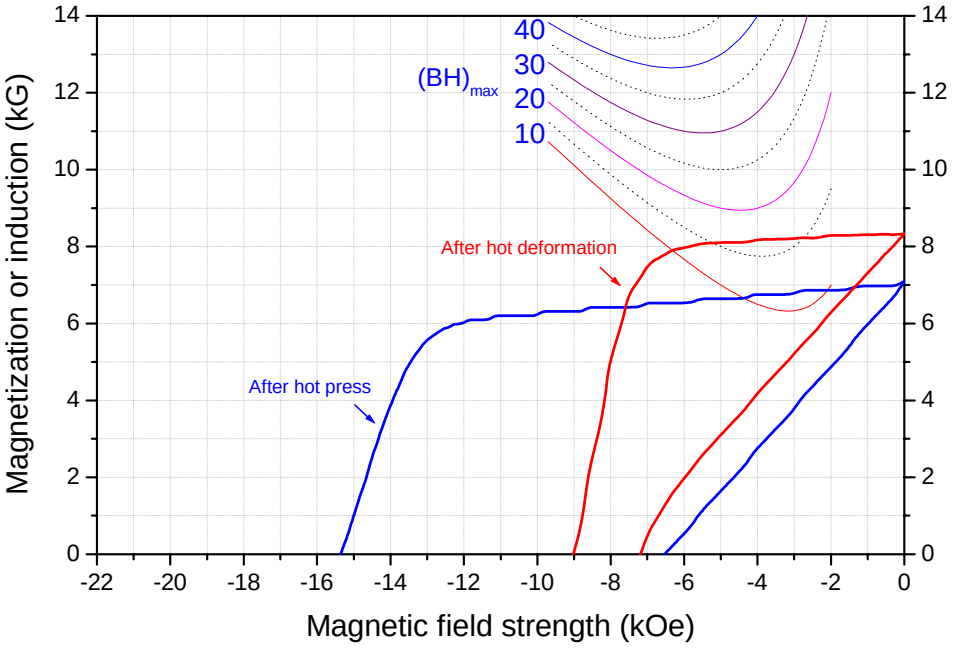

Fig. 10. Demagnetization curves of hot pressed isotropic $PrCo_5$ and hot deformed anisotropic $PrCo_5$.

Demagnetization curves of the first hybrid $Pr_2(Fe_{0.94}Co_{0.06})_{14}B/PrCo_5$ [80 wt%/20 wt%] magnet is shown in Figure 11. Its magnetic performance is beyond our expectation. This specimen has a high ${}_MH_c$ over 16 kOe and $(BH)_{max}$ near 33 MGOe. Figure 12 demonstrates magnetic properties as a function of the fraction of the $PrCo_5$ component in the hybrid

$Pr_2(Fe_{0.94}Co_{0.06})_{14}B/PrCo_5$ magnet. Figure 12 also indicates that when the fraction of $PrCo_5$ is increased to 40 wt% in the hybrid magnet, $(BH)_{max}$ dropped to around 24 MGOe, basically as a result of the drop of $_MH_c$. As mentioned previously, since intrinsic coercivity higher than that of $Pr_2(Fe,Co)_{14}B$ should be developed in $PrCo_5$, much better magnetic properties can be achieved in hybrid magnets with a high fraction of $PrCo_5$.

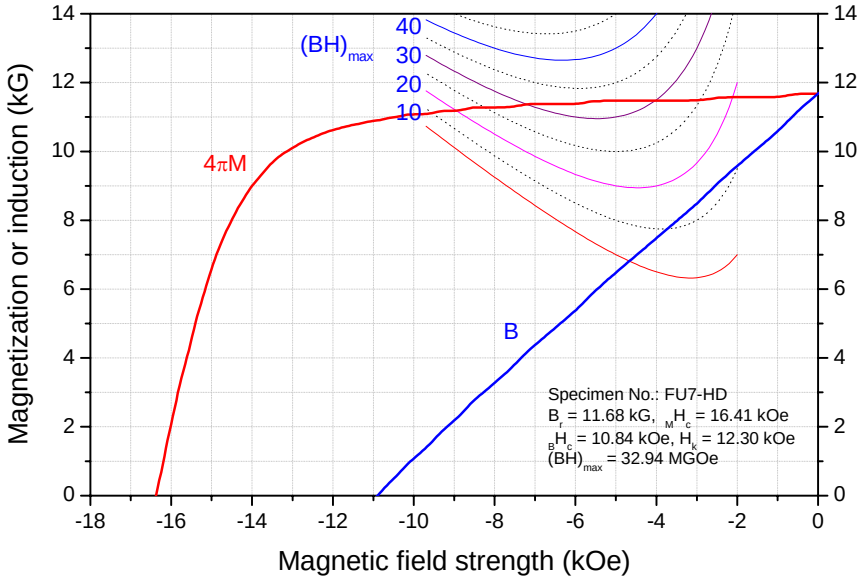

Fig. 11. Demagnetization curves of the 1st bulk hot deformed nanocrystalline $Pr_2(Fe_{0.94}Co_{0.06})_{14}B/PrCo_5$ [80 wt%/20 wt%].

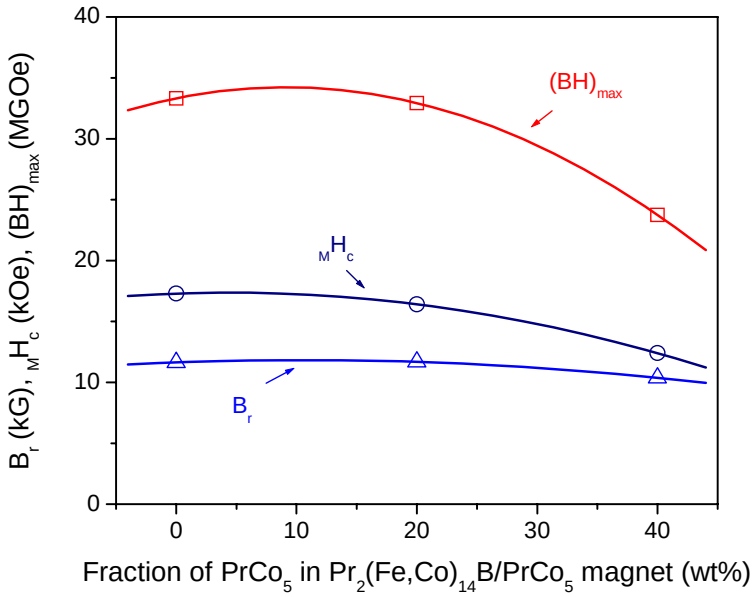

Fig. 12. Magnetic properties as a function of the fraction of $PrCo_5$ in hybrid $Pr_2(Fe_{0.94}Co_{0.06})_{14}B/PrCo_5$ magnet.

Partial substitution of Fe for Co in $PrCo_5$ was made to increase its magnetization and, hence, energy product. Figure 13 shows demagnetization curves of a hybrid nanocrystalline $Pr_2(Fe_{0.94}Co_{0.06})_{14}B/Pr(Co_{0.8}Fe_{0.2})_5$ [80 wt%/20 wt%] magnet. The B_r of this hybrid magnet was increased to 12 kG and $(BH)_{max}$ was increased to 34.5 MGOe. At the same time, its intrinsic coercivity increased to near 17 kOe, which also beyond our anticipation.

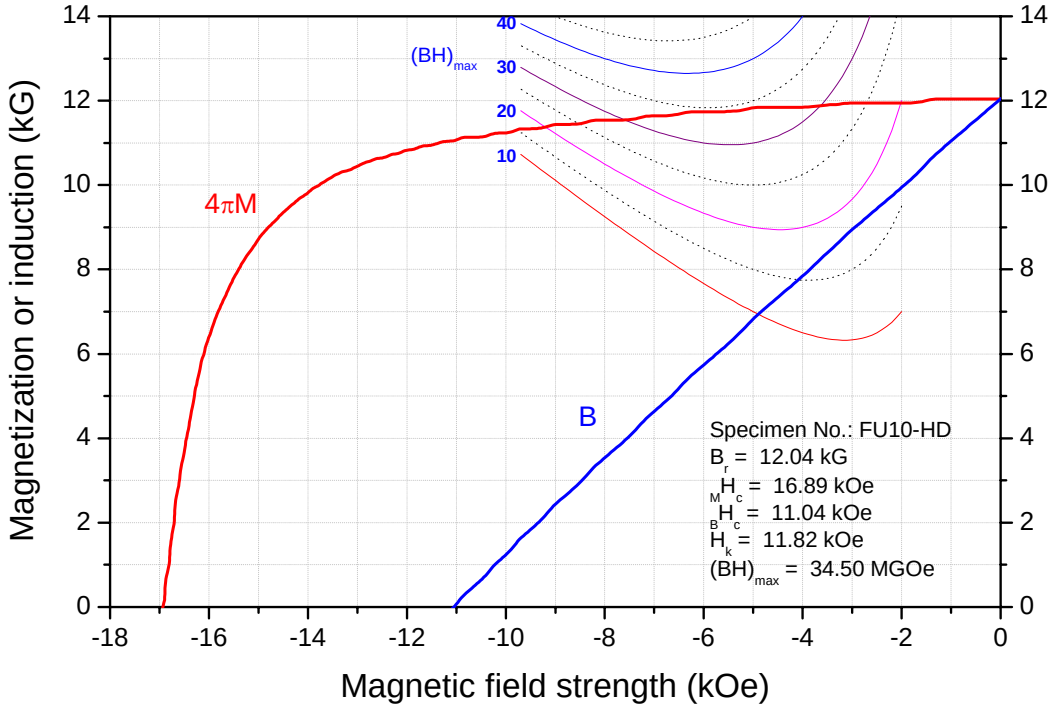

Fig. 13. Demagnetization curves of the 1st bulk hot deformed nanocomposite $Pr_2(Fe_{0.94}Co_{0.06})_{14}B/Pr(Co_{0.8}Fe_{0.2})_5$ [80 wt%/20 wt%].

Figure 14 shows the temperature coefficient of magnetic flux versus temperature for (1) $Pr_2(Fe_{0.94}Co_{0.06})_{14}B$; (2) $Pr(Co_{0.8}Fe_{0.2})_5$; (3) hybrid nanocrystalline $Pr_2(Fe_{0.94}Co_{0.06})_{14}B/Pr(Co_{0.8}Fe_{0.2})_5$ [80 wt%/20 wt%]; and (4) $Pr_2(Fe_{0.94}Co_{0.06})_{14}B/Pr(Co_{0.8}Fe_{0.2})_5$ [60 wt%/40 wt%]. Assuming that a temperature coefficient of not worse than -0.10%/°C is required for a particular application, to satisfy this requirement, the highest operating temperature for $Pr_2(Fe_{0.94}Co_{0.06})_{14}B$ is only 40°C. The operating temperatures can be increased to 90°C and 175°C, respectively, if the hybrid $Pr_2(Fe_{0.94}Co_{0.06})_{14}B/Pr(Co_{0.8}Fe_{0.2})_5$ [80 wt%/20 wt%] and $Pr_2(Fe_{0.94}Co_{0.06})_{14}B/Pr(Co_{0.8}Fe_{0.2})_5$ [60 wt%/40 wt%] are used.

Figure 15 shows SEM micrographs of an anisotropic hybrid $Pr_2(Fe_{0.94}Co_{0.06})_{14}B/Pr(Co_{0.8}Fe_{0.2})_5$ [60 wt%/40 wt%] magnet. It can be seen from Figure 15(a) that the grain size in this magnet is not uniform. In addition to small grains, there are some large grains in micron range. Figure 15(b) is a high resolution SEM image showing elongated and aligned grains. However, the long axes of some grains are over 500 nm. With further reductions in the grain size, better magnetic performance is anticipated.

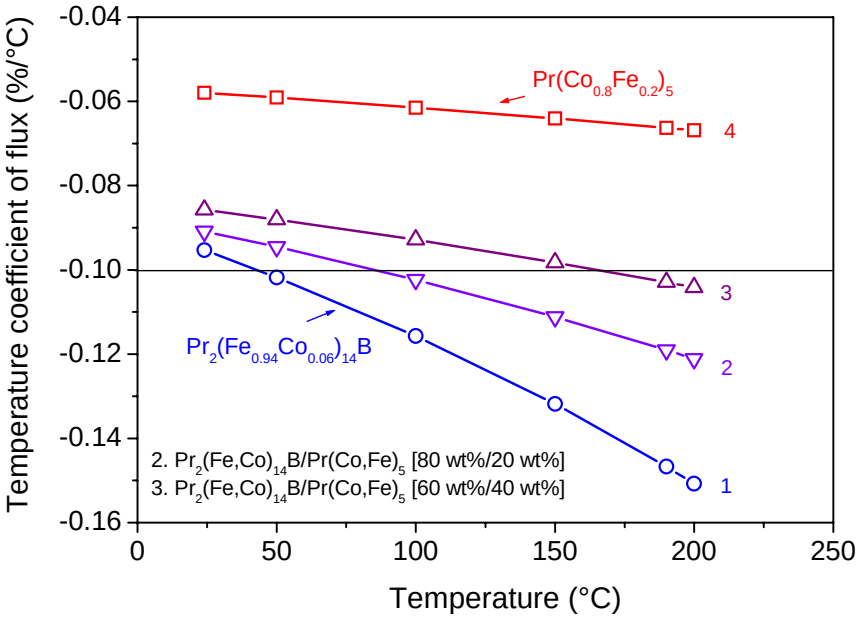

Fig. 14. Temperature coefficient of magnetic flux versus temperature for (1) $Pr_2(Fe_{0.94}Co_{0.06})_{14}B$; (2) hybrid $Pr_2(Fe_{0.94}Co_{0.06})_{14}B/Pr(Co_{0.8}Fe_{0.2})_5$ [80 wt%/20 wt%]; (3) hybrid $Pr_2(Fe_{0.94}Co_{0.06})_{14}B/Pr(Co_{0.8}Fe_{0.2})_5$ [60 wt%/40 wt%]; and (4) $Pr(Co_{0.8}Fe_{0.2})_5$.

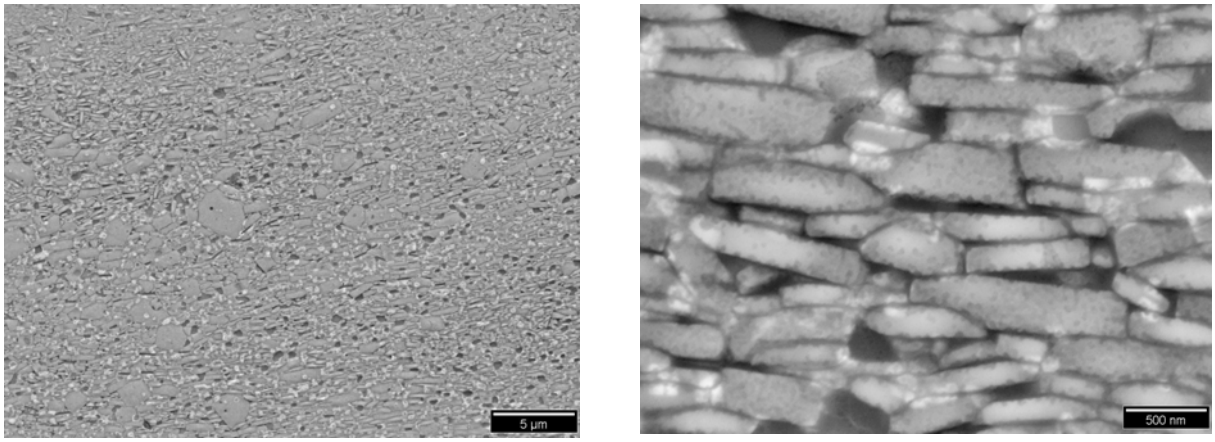

(a) (b)

Fig. 15. SEM micrographs of anisotropic hybrid $Pr_2(Fe_{0.94}Co_{0.06})_{14}B/Pr(Co_{0.8}Fe_{0.2})_5$ [60 wt%/40 wt%].

As mentioned previously, partial substitution of Fe for Co in $PrCo_5$ was made to increase its magnetization and, hence, energy product. This substitution leads to a sharp drop of ${}_MH_c$ and $(BH)_{max}$ of $PrCo_5$ as shown in Figure 16. Surprisingly, it was observed that for the hybrid nanocrystalline $Pr_2(Fe_{0.94}Co_{0.06})_{14}B/Pr(Co_{1-x}Fe_x)_5$ [80 wt%/20 wt%], the Fe substitution results in increased ${}_MH_c$ and $(BH)_{max}$. As shown in Figure 17, the ${}_MH_c$ of the hybrid magnet reaches 17.3 KOe when x = 0.3. At the same time, the magnet remains a high $(BH)_{max}$ of 34.2 MGOe.

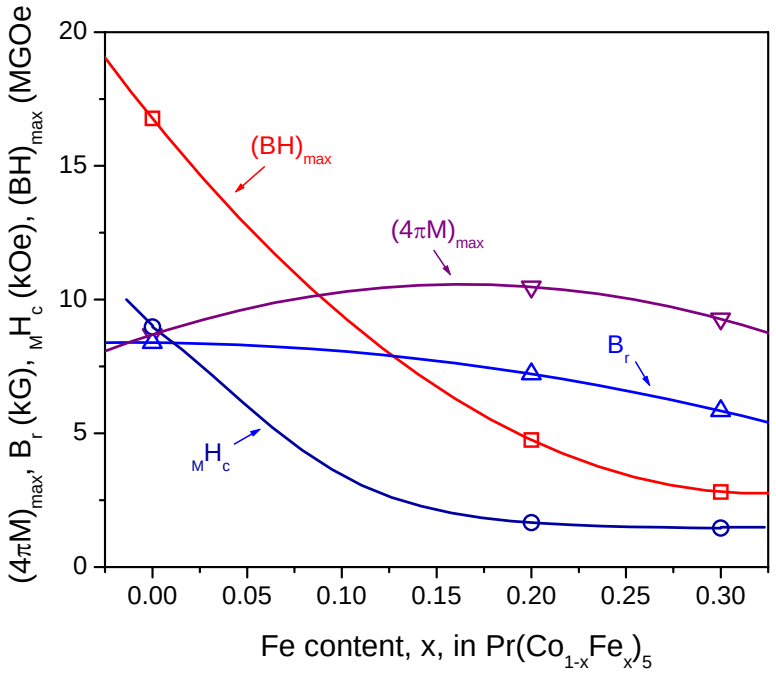

Fig. 16. Effect of Fe content, x, in $Pr(Co_{1-x}Fe_x)_5$ on magnetic properties of $Pr(Co_{1-x}Fe_x)_5$.

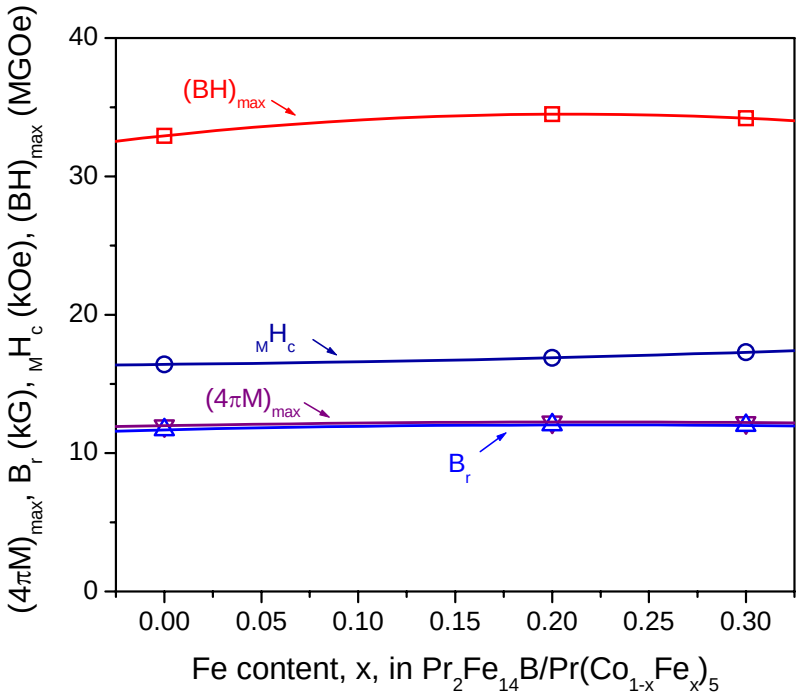

Fig. 17. Effect of Fe content, x, in $Pr_2(Fe,Co)_{14}B/Pr(Co_{1-x}Fe_x)_5$ on $(4\pi M)_{max}$, B_r, $_MH_c$, and H_k of hybrid nanocrystalline $Pr_2(Fe,Co)_{14}B/Pr(Co_{1-x}Fe_x)_5$.

In addition, an abnormal increase of $_MH_c$ after hot deformation in the hybrid nanocrystalline $Pr_2(Fe,Co)_{14}B/Pr(Co,Fe)_5$ system was observed. In a normal case, after a hot pressed isotropic magnet is further hot deformed to an anisotropic magnet, its $_MH_c$ will be decreased 20 to 40% as a result of grain growth, as shown in Figures 9 and 10. However, an increase of $_MH_c$ in the hybrid nanocrystalline $Pr_2(Fe,Co)_{14}B/Pr(Co,Fe)_5$ system was observed after hot deformation as shown in Figures 18 and 19. It can be seen from Figure 19 that the hot pressed isotropic $Pr_2(Fe_{0.94}Co_{0.06})_{14}B/Pr(Co_{0.7}Fe_{0.3})_5$ [60 wt%/40 wt%] has a low $_MH_c$ value of 8.5 kOe. However, after hot deformation, its $_MH_c$ was increased to 17 KOe! This abnormal enhancement of $_MH_c$ may have the same origin as the $_MH_c$ increase shown in Figure 17. It certainly related to the interaction between $Pr_2(Fe,Co)_{14}B$ and $Pr(Co,Fe)_5$ phases.

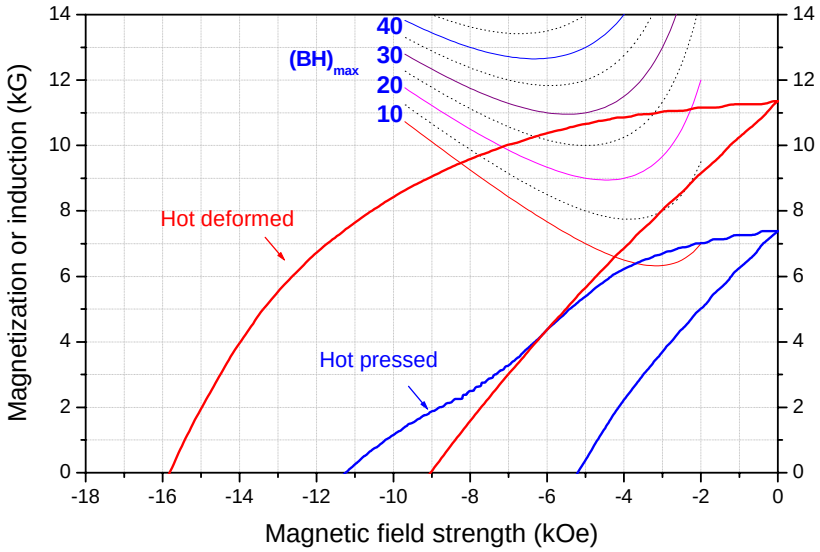

Fig. 18. Demagnetization curves of hot pressed and hot deformed $Pr_2(Fe_{0.94}Co_{0.06})_{14}B/Pr(Co_{0.8}Fe_{0.2})_5$ [60 wt%/40 wt%].

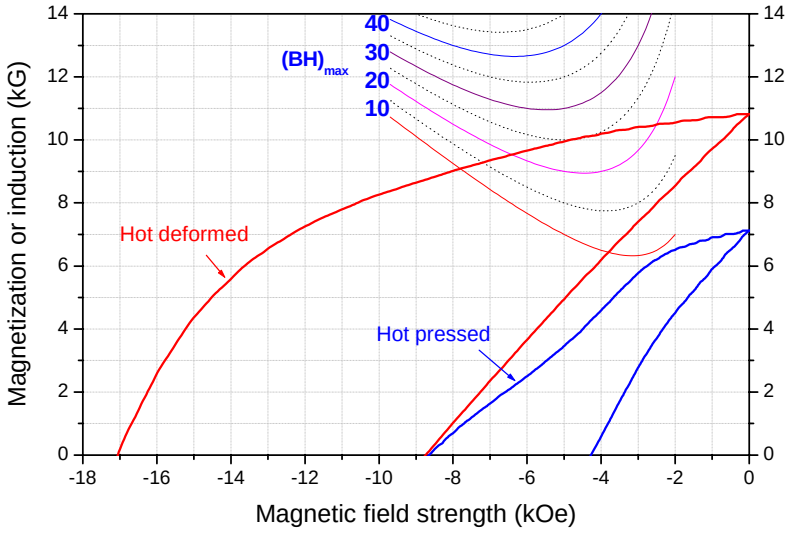

Fig. 19. Demagnetization curves of hot pressed and hot deformed $Pr_2(Fe_{0.94}Co_{0.06})_{14}B/Pr(Co_{0.7}Fe_{0.3})_5$ [60 wt%/40 wt%].

One possible reason may be that because the inductive hot press was performed at a relatively low temperature of 600°C for only 2 minutes, the amorphous $Pr_2(Fe,Co)_{14}B$/ $Pr(Co,Fe)_5$ powder may be only partially crystallized after the hot press, leading to low coercivity. After subsequent hot deformation, the magnet alloy is fully crystallized and thus demonstrates increased coercivity. However, the x-ray diffraction (XRD) analyses did not give strong support to this assumption. Figure 20 shows the XRD pattern of the as-mechanically alloyed powder of $Pr_2(Fe_{0.94}Co_{0.06})_{14}B/Pr(Co_{0.7}Fe_{0.3})_5$ [60 wt%/40 wt%]. It is in an amorphous condition except for an α-Fe peak. The XRD pattern of the same alloy powder after the hot press is given in Figure 21. Basically, the amorphous powder is crystallized after the hot press, though it has very fine grain structure as indicated by the wide half-peak width as shown in Figure 21.

Therefore, the abnormal enhancement of coercivity, as indicated in Figures 17 through 19 remains unknown and it will be an interesting subject to be studied in the STTR Phase II project.

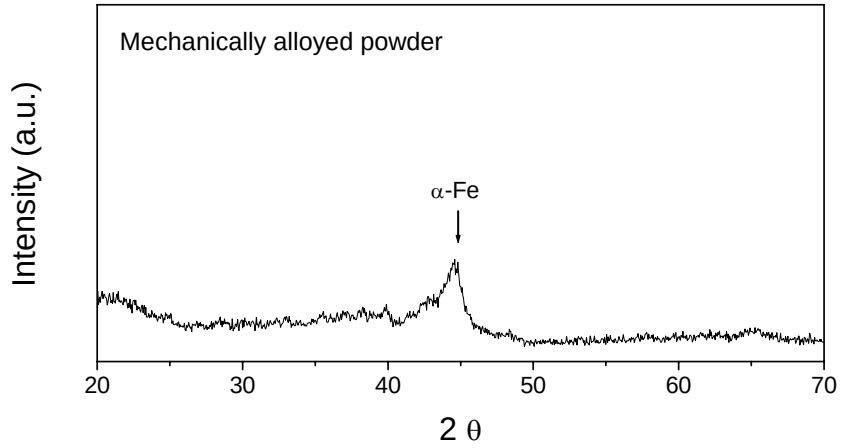

Fig. 20. XRD pattern of a powder mixture of $Pr_2(Fe_{0.94}Co_{0.06})_{14}B/Pr(Co_{0.7}Fe_{0.3})_5$ [60 wt%/40 wt%] after mechanical alloying.

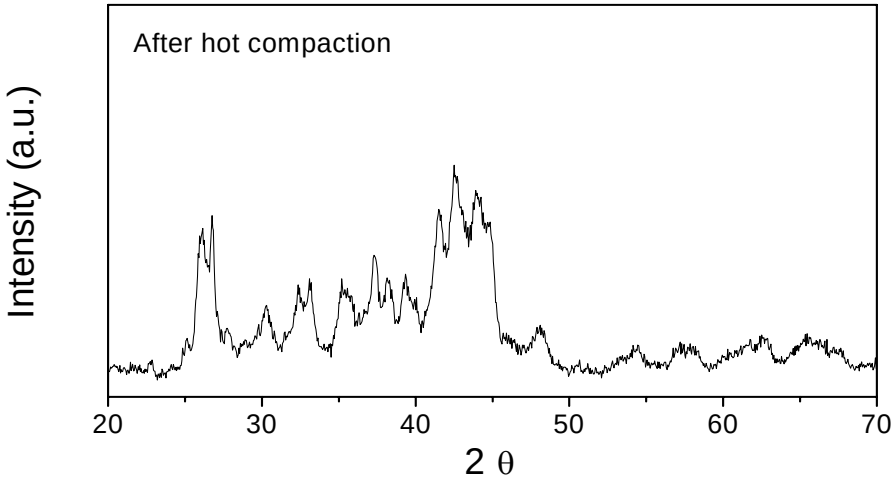

Fig. 21. XRD pattern of hot compacted $Pr_2(Fe_{0.94}Co_{0.06})_{14}B/Pr(Co_{0.7}Fe_{0.3})_5$ [60 wt%/40 wt%].

5. Anticipated Public Benefits

Based on accomplishments made by the FutureTek/University of Dayton research team in the successful STTR Phase I project, it is highly anticipated that after further research a commercial product of a new class of hybrid nanograin $Pr_2(Fe,Co)_{14}B$ /$Pr(Co,Fe)_5$ permanent magnets will be developed. In the Phase I project, high intrinsic coercivity of 16.4 kOe and high energy product of 32.9 MGOe were obtained in the very first hybrid nanograin magnet of $Pr_2(Fe_{0.94}Co_{0.06})_{14}B/PrCo_5$ [80 wt%/20 wt%]. Shortly afterwards, $_MH_c$ = 17 kOe and $(BH)_{max}$ = 35 MGOe were achieved in a hybrid nanograin $Pr_2(Fe_{0.94}Co_{0.06})_{14}B/ Pr(Co_{0.8}Fe_{0.2})_5$ [80 wt%/20 wt%] magnet. The FutureTek/University of Dayton researchers are confident that through further research and development, innovative technologies and cost-effective manufacturing processes for synthesizing hybrid nanocrystalline $Pr_2(Fe,Co)_{14}B/Pr(Co,Fe)_5$ magnets with $(BH)_{max}$ = 35 - 45 MGOe will be developed. Compared with the current commercial Nd-Fe-B magnets, new hybrid magnets will have:

- The same level of magnetic performance as compared with the mainstream sintered $Nd_2Fe_{14}B$ magnets that have $(BH)_{max}$ in the range of 35 to 45 MGOe. At the same time, new magnets have significantly improved thermal stability.
- Magnetic performance about 27% higher than that of the commercial $(Nd,Dy,Tb)_2(Fe,Co)_{14}B$ magnets currently used for elevated temperature applications as a result of eliminating heavy rare earths Dy and Tb.
- Higher Curie temperature of around 500°C and improved temperature coefficients of B_r, $_MH_c$, and $(BH)_{max}$ as a result of utilizing the thermally stable $Pr(Co,Fe)_5$ phase.
- Higher operating temperature up to 250°C or higher. This temperature is 170°C higher than mainstream $Nd_2Fe_{14}B$ magnets and 100°C higher than $(Nd,Dy,Tb)_2(Fe,Co)_{14}B$ magnets.
- Potentially lower cost than commercial $(Nd,Dy,Tb)_2(Fe,Co)_{14}B$ because of eliminating expensive Dy and Tb and simple processing.
- Capability to be used for very low temperature applications. In comparison, $Nd_2Fe_{14}B$-based magnets cannot be used at temperatures lower than -130°C because of spin reorientation. $Pr_2(Fe,Co)_{14}B/Pr(Co,Fe)_5$ does not have spin reorientation.

A comparison of proposed hybrid nanograin magnets with conventional Nd-Fe-B magnets is given in Table 2.

Table 2. Comparison of Conventional Nd-Fe-B Magnets and Proposed $Pr_2(Fe,Co)_{14}B/Pr(Co,Fe)_5$ Magnets

Magnet	$(BH)_{max}$ (MGOe)	Curie Point (°C)	Absolute Value of Temperature Coefficients of B_r, $_MH_c$ and $(BH)_{max}$	Upper Operating Temperature (°C)
Mainstream $Nd_2Fe_{14}B$-based Magnets	35 - 45	310	Large	80
Commercial $(Nd,Dy,Tb)_2(Fe,Co)_{14}B$	28 - 35	350	Large	150°C
Proposed $Pr_2(Fe,Co)_{14}B/Pr(Co,Fe)_5$	35 - 45	500	Small	250°C or higher

Combining high magnetic performance and excellent thermal stability, this new class of hybrid nanograin magnets possesses tremendous technical, economic, and social significance. When used for beam focusing in high-energy accelerators, the magnet's resistance to the radiation damage will be significantly improved, since the nature of the radiation damage is virtually a radiation-induced thermal effect as previously.

The market of permanent magnet is of multi-billion US dollars per year. Figure 22 gives information on the world-wide market for permanent magnets, estimated to be $7 billion in 2002. Among all permanent magnets, hard ferrites account for about $4 billion, and rare earth magnets for $2.5 billion, of which Nd-Fe-B and Sm-Co are $1.8 and $0.7 billion, respectively. Nd-Fe-B magnets are now widely used in the electronics, communications, transportation, and medical instrument industries. It is estimated that the world output of Nd-Fe-B magnets is increasing at more than 12% per year.

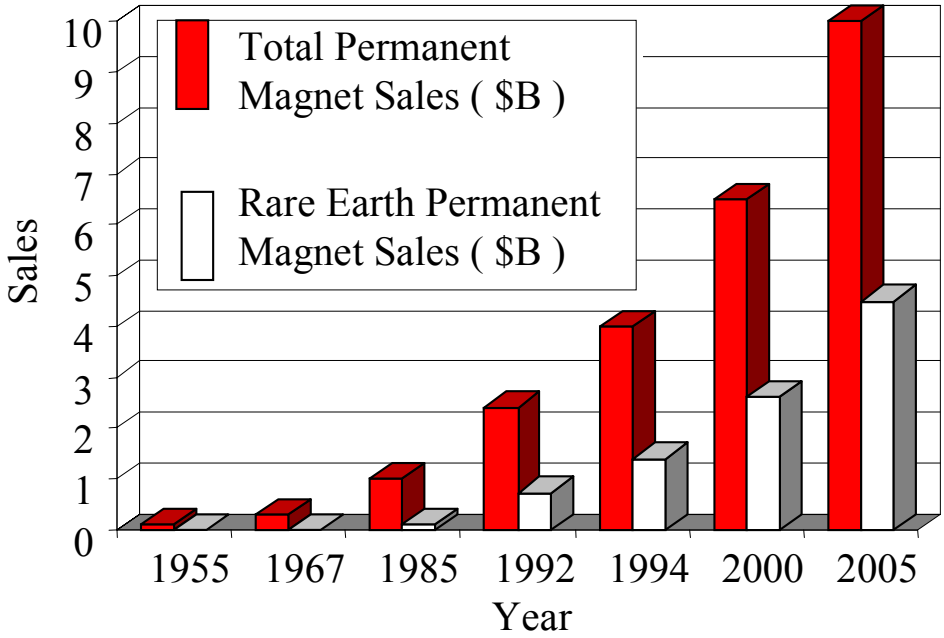

Fig. 22. Permanent magnet market.

A trend toward electrical propulsion has developed in recent years. Associated with this trend, more electrical automobiles and other vehicles, more electrical aircraft, and more electrical ships will gradually emerge into our life. The advantages of applying more electrical propulsion include (1) enhanced energy efficiency and productivity; (2) reduced dependence on fossil fuels and foreign energy resources; (3) reduced air pollution; (4) reduced hydraulic control system; and (5) improved system reliability and maintainability. More electrical propulsion (and all electrical propulsion in the future) imposes an urgent need for advanced permanent magnet materials with good thermal stability beyond current Nd-Fe-B magnets.

The new class of hybrid nanocrystalline magnets has emerged as the times demand. They have the same level of magnetic performance as the mainstream Nd-Fe-B, but much improved thermal stability, which fills the operating temperature gap and addresses the thermal stability issues between Sm-Co and Nd-Fe-B magnets. The new magnets can fulfill Federal Government and commercial sector requirements in many applications, such as:

- DoE high energy accelerator program for beam focusing in electron linear accelerators, and solenoids for use in electron-beam or ion-beam sources or for klystron or other radio frequency amplifier tubes operating at wavelengths from 0.7 to 10 cm. Promote novel device and instrumentation development.
- DoE FreedomCAR and Vehicle Technologies program for hybrid and fuel-cell-powered vehicle applications.
- DoE and DoD magnetic sensor applications where a very small temperature coefficient of magnetic properties is required.
- DoD navigation system of aircraft and smart bombs.
- NASA spacecraft propulsion and navigation.
- Advanced motors, generators, and actuators.

6. References

1. J T Volk. "Summary of Radiation Damage Studies on Rare Earth Permanent Magnets," http://home.fnal.gov/~volk/.
2. C.H. Chen, J. Talnagi, J. Liu, P. Vora, A. Higgins, and S. Liu, "The Effect of Neutron Irradiation on Sm_2Co_{17}-Based High Temperature Magnets and Nd-Fe-B Magnets," presented at 2005 International Conference on Magnetics, Nagoya, Japan, April 4-8, 2005.
3. S. Liu, B. Cui, S. Bauser, R. Leese, J.S. Hilton, R.H. Yu, A. Kramp, J. Dent, and D. Miles, "Approach to synthesizing bulk, fully dense anisotropic nanocomposite rare earth permanent magnets," *Proc. 17th Int'l. Workshop on REPM*, 939 (2002).
4. S. Liu, "Effect of Nanograin Structure on Magnetic Properties of Rare Earth Permanent Magnets," *Proc. Int'l. 18th Workshop on HPM* 2, 690 (2004).
5. D. Lee, J.S. Hilton, S. Liu, Y. Zhang, G.C. Hadjipanayis, and C.H. Chen, "Hot-Pressed and Hot-Deformed Nanocomposite $(Nd,Pr,Dy)_2Fe_{14}B/\alpha$-Fe-based Magnets," *IEEE Trans. Magn.* 39, 2947 (2003).

6. D. Lee, J.S. Hilton, C.H. Chen, M.Q. Huang, Y. Zhang, G.C. Hadjipanayis, and S. Liu, "Bulk Isotropic and Anisotropic Rare Earth Magnets," to be published in *IEEE Trans. Magn.* 40 (2004).

7. Senno and Y. Tawara, "Permanent-Magnet Properties of Sm-Ce-Co-Fe-Cu Alloys with Compositions Between 1-5 and 2-17," *IEEE Trans. Magn*. 10, 313 (1974).

8. T. Ojima, S. Tomizawa, T. Yoneyama, and T. Hori, "Magnetic Properties of a New Type of Rare-Earth Cobalt Magnets $Sm_2(Co, Cu, Fe, M)_{17}$," *IEEE Trans. Magn*. 1, 1317 (1977).

9. A.E. Ray, W.A. Soffa, J.R. Blachere, and B. Zhang, "Cellular Microstructure Development in $Sm(Co,Fe,Cu,Zr)_{8.35}$ Alloys," *IEEE Trans. Magn*. 23, 2711 (1987).

10. B.Z. Cui, M.-Q. Huang, and S. Liu, "Magnetic Properties of $SmCo_7$/Co and $Sm(Co,Fe)_7\alpha$-(Fe,Co) Nanocomposite Magnets Prepared by Magnetic Annealing," *IEEE Trans. Magn.* 39, 2866 (2003).

11. G.I. Hoffer and K.J. Strnat, "Magnetocrystalline Anisotropy of YCo_5 and Y_2Co_{17}," *IEEE Trans. Magn.* 2, 487 (1966).

12. C.H. Chen, M.H. Walmer, D. Lee, S. Liu, Y. Zhang, and G. Hadjipanayis, "Fully Dense Nanocomposites of $(Sm,Gd)_2(Co,Fe)_{17}$ + (Co,Fe) with High Coercivity, High T_c, and Low Temperature Coefficient" *IEEE Trans. Magn*. 40 (5), 2928 (2004).

13. M.Q. Huang, Z. Turgut, B. Wheeler, D. Lee and S. Liu, Z.M. Chen and B.M. Ma, Y.G. Peng, S.Y. Chu, and D.E. Laughlin, J. C. Horwath and R. T. Fingers, "Fully Dense Anisotropic Nanocomposite $Sm(Co,Fe,Zr,Cu,B)_z$ (z=7.5-12) Magnets," Presented at the Annual Conference of Magnetism and Magnetic Materials," Tampa, FL, 2004.